

H-induced effects in luminescent silicon nanostructures obtained from plasma enhanced chemical vapor deposition grown $\text{Si}_y\text{O}_{1-y}:\text{H}$ ($y > 1/3$) thin films annealed in (Ar+5% H_2)

D. Comedi,^{a)} O. H. Y. Zalloum, E. A. Irving, J. Wojcik, and P. Mascher
Centre for Emerging Device Technologies, Department of Engineering Physics, McMaster University,
Hamilton, Ontario L8S 4L7, Canada

(Received 19 August 2005; accepted 23 January 2006; published 4 May 2006)

$\text{Si}_y\text{O}_{1-y}:\text{H}$ ($y=0.36$ and 0.42) alloy films were fabricated by electron cyclotron resonance plasma enhanced chemical vapor deposition and subsequently annealed in (Ar+5% H_2) at different temperatures. Glancing angle x-ray diffraction and Fourier transform infrared spectroscopy measurements revealed the formation of silicon nanoclusters (Si-ncl) in an amorphous SiO_2 matrix for films annealed at temperatures of 900 °C and above. Negligible photoluminescence (PL) was observed at room temperature for the as-grown samples; however, PL bands appeared in the visible after the annealing treatments. The PL intensities are much higher and the spectra skewed to the red as compared to data obtained for similar samples annealed in pure Ar. These effects are attributed to the passivation by H atoms of nonradiative recombination centers in the materials annealed in (Ar+5% H_2). The overall analysis of the PL data indicates that both quantum confinement and defect states contribute to the luminescence. Two-step annealing procedures [in Ar and then in (Ar+5% H_2)] were found to yield slightly higher passivation efficiencies than single annealing steps in (Ar+5% H_2). © 2006 American Vacuum Society. [DOI: 10.1116/1.2177227]

I. INTRODUCTION

When substoichiometric silicon oxide alloys ($\text{Si}_y\text{O}_{1-y}$, where $y > 1/3$ and typically $y < 0.5$) are annealed at temperatures of 900 °C and above, a stoichiometric SiO_2 phase gradually forms while the excess Si ($y - 1/3$) precipitates.¹⁻³ For sufficiently small values of y , Si clusters of nanometer range size (Si-ncl) embedded in an amorphous SiO_2 are obtained. The mean Si-ncl size increases with increasing y , annealing temperature (T), and/or annealing duration (t).^{3,4} This system is very promising for silicon-based photonics⁵ since it exhibits efficient photoluminescence (PL) in the visible whose intensity and energy depend on the Si-ncl size. The effect has been often explained in terms of a quantum confinement (QC) effect,^{1,2,5} where efficient light emission occurs due to exciton recombination across a size-dependent Si-ncl band gap. In real systems, however, the presence of electronic states at the Si-nc/ SiO_2 interface region may be important in the light emission process as well.⁶⁻⁸ It is well known that this region is not spatially sharp and that it contains undercoordinated atoms [i.e., dangling bonds (dbs)]. A single db is sufficient to deactivate light emission from a Si-ncl due to the large electron-hole capture cross section of this defect.⁹ Hence it is important to study and establish different passivation schemes in order to fully exploit the potential of this promising luminescent system.

Although H has been used before¹⁰ to passivate defects in some Si-ncl/ SiO_2 systems, its effects on the luminescence are not well understood. In this work, we study the structure and PL of Si-ncls embedded in a SiO_2 matrix that result from

the annealing in (Ar+5% H_2) of $\text{Si}_y\text{O}_{1-y}:\text{H}$ alloy films fabricated by electron cyclotron resonance plasma enhanced chemical vapor deposition (ECR-PECVD).

II. EXPERIMENT

The $\text{Si}_y\text{O}_{1-y}:\text{H}$ films ($y=0.36$ and 0.42 , 2 μm thick) were deposited on (100) c -Si substrates held at 120 °C using an ECR-PECVD reactor described elsewhere.¹¹ The silicon content y was determined by Rutherford backscattering measurements. Annealing of the samples was performed in a quartz tube furnace under either Ar or (Ar+5% H_2) atmospheres for times from 30 min to 3 h and at temperatures between 800 and 1100 °C. PL measurements were carried out in the 400–1000 nm range at room temperature using the 325 nm line of a He–Cd laser and an Ocean Optics spectrometer. The effective power density of the laser beam on the surface of the samples was ~ 0.64 W/cm². All PL spectra were corrected for the detection system response and converted into photon flux spectra. X-ray diffraction (XRD) scans were performed using the $\text{Cu } K\alpha$ line in a Bede D1 diffractometer at a fixed (2.5°) beam incidence angle with respect to the film surface. This angle is well above the critical angle for total external reflection. It was chosen so as to fix and increase the probed effective oxide film thickness by a factor of $\sin(\theta)/\sin(2.5^\circ)$ with respect to the thickness that would otherwise be probed in a symmetric diffraction scan through the Bragg angle θ , while keeping the illuminated area restricted to the typical sample size of 2 cm². The bonding structure of the as-grown and annealed samples was studied by transmission Fourier transform infrared (FTIR) spectroscopy in the 4000–350 cm⁻¹ wave number range.

^{a)}Electronic mail: comedid@mcmaster.ca

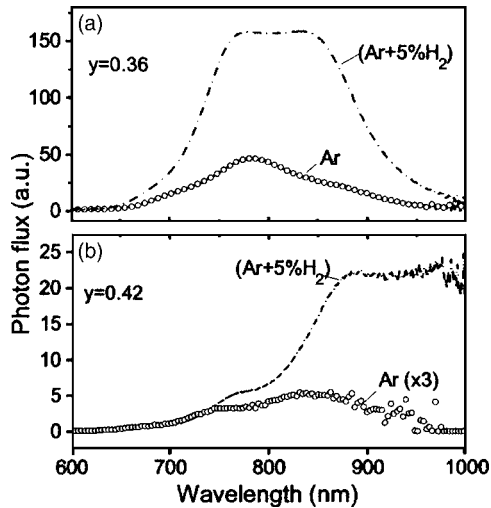


FIG. 1. PL spectra converted to photon flux spectra as measured for $\text{Si}_y\text{O}_{1-y}:\text{H}$ with (a) $y=0.36$ and (b) $y=0.42$ annealed in $(\text{Ar}+5\% \text{H}_2)$ (lines) and Ar (symbols).

III. RESULTS

Figures 1(a) and 1(b) show PL spectra obtained for $\text{Si}_{0.36}\text{O}_{0.64}$ and $\text{Si}_{0.42}\text{O}_{0.58}$ samples, respectively, annealed in Ar and $(\text{Ar}+5\% \text{H}_2)$ for 3 h at 1100°C . The spectra for the unannealed samples do not exhibit any appreciable signal and are not shown. It can be seen that after annealing in Ar, broad PL bands that peaked at about 784 and 841 nm are obtained for $y=0.36$ and 0.42, respectively. In addition, the PL intensity is seen to be significantly lower for the $y=0.42$ case. It is well known that usually larger Si-ncs form^{1,3} in materials with larger y , which should lead to weaker QC and consequently a narrower Si-nc band gap. Therefore, the redshift and lower intensity observed for $y=0.42$ as compared to $y=0.36$ are qualitatively consistent with the predictions of the QC effect. As can also be noted in Figs. 1(a) and 1(b), significant modifications of the PL bands occur when the annealing is performed in $(\text{Ar}+5\% \text{H}_2)$ as compared to pure Ar. First, the integrated PL intensity increases by several hundreds of percent in both cases, the increase being larger for the larger y material. Second, the PL bands for both samples skew to the red with respect to the Ar annealing case. We attribute these effects to the passivation of nonradiative recombination centers, such as Si dangling bonds at the Si-nc/SiO₂ interface region, by H atoms incorporated during the annealing.

Figure 2 shows XRD curves in the region of the Si (111) peak obtained for the $y=0.42$ samples annealed in $(\text{Ar}+5\% \text{H}_2)$ at three different temperatures. It can be seen that as T increases, two peaks develop in the XRD patterns. The first one is broad and located close to 21° . It characterizes an α -SiO₂ phase with varying degrees of medium range order.³ The second peak appears at about 28° and it is due to the Si (111) planes. Weaker peaks corresponding to the Si (220) and (311) planes are also detected (not shown here). Hence, the XRD data show that the annealing in $(\text{Ar}+5\% \text{H}_2)$ of the silicon-rich silicon oxide (SRSO) leads to the separation of

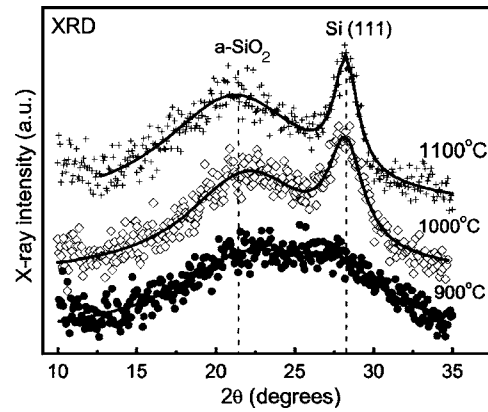


FIG. 2. X-ray diffraction patterns for $\text{Si}_y\text{O}_{1-y}:\text{H}$ with $y=0.42$ annealed in $(\text{Ar}+5\% \text{H}_2)$ at 900°C (closed circles), 1000°C (open diamonds), and 1100°C (crosses).

the α -SiO₂ and Si phases and to the crystalline Si-nc formation. As can also be seen in Fig. 2, the Si (111) peak narrows as T increases from 1000 to 1100°C . Using the Scherrer formula,^{3,12} this change indicates an increase of the mean size of Si precipitates from 3.5 to 5.2 nm. Samples annealed in pure Ar were also thoroughly studied by XRD and no significant differences with respect to the effects observed for identical samples annealed in $(\text{Ar}+5\% \text{H}_2)$ at the same T and t could be detected. We hence conclude that the inclusion of 5% H_2 in the annealing gas does not influence the gross features of Si-nc growth kinetics.

Further evidence for this conclusion is obtained from the PL study itself. Figures 3(a) and 3(b) show the data from Figs. 1(a) and 1(b) as compared to PL spectra for samples that were annealed in pure Ar (1100°C , 3 h) first and then posthydrogenated in $(\text{Ar}+5\% \text{H}_2)$ for 2 h at various $T < 1100^\circ\text{C}$. PL studies of samples annealed in pure Ar at

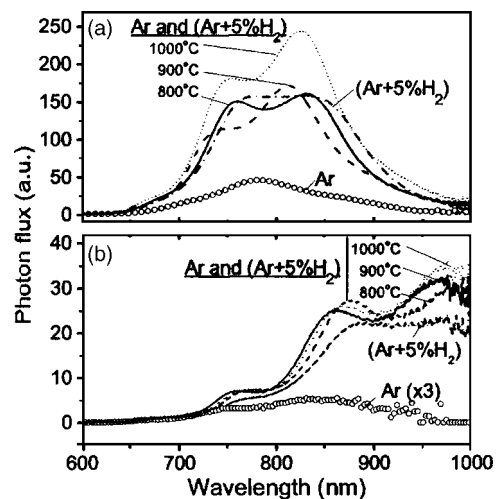


FIG. 3. PL spectra converted to photon flux spectra as measured for $\text{Si}_y\text{O}_{1-y}:\text{H}$ with (a) $y=0.36$ and (b) $y=0.42$ annealed in $(\text{Ar}+5\% \text{H}_2)$ (solid lines) and Ar (symbols). Also shown are spectra obtained for similar samples annealed in Ar (3 h, 1100°C) and then for 2 h in $(\text{Ar}+5\% \text{H}_2)$ at 800°C (dashed lines), 900°C (dashed-dotted lines), and 1000°C (dotted lines).

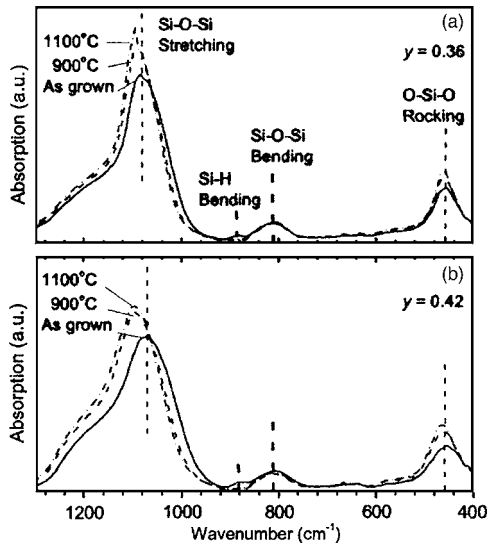


FIG. 4. Absorption spectrum in the infrared for the $\text{Si}_y\text{O}_{1-y}:\text{H}$ samples with (a) $y=0.36$ and (b) $y=0.42$ annealed in ($\text{Ar}+5\% \text{H}_2$) at 900°C (dashed lines) and 1100°C (dashed-dotted lines). The spectra for the as-grown samples are also shown as solid lines.

1100°C show that the PL intensity nearly saturates for $t > 1$ h for both Si contents, indicating that the phase separation process is essentially completed. As can be seen in Figs. 3(a) and 3(b), the posthydrogenation step produces similar gross changes in the PL spectra as the annealing of as-grown samples in ($\text{Ar}+5\% \text{H}_2$) (i.e., increase of the intensity and skew of the spectra to the red as compared to annealing in pure Ar). We note, in addition, that the posthydrogenation temperature has some effect on the PL intensity, which is found to be the highest at 1000°C , more clearly seen for $y=0.36$.

Figure 4 shows the FTIR spectra obtained for the as-grown $y=0.36$ and $y=0.42$ films after annealing in ($\text{Ar}+5\% \text{H}_2$) at 900 and 1100°C . The Si–O–Si stretching, Si–O–Si bending, and O–Si–O rocking modes can be observed at 1080 , 812 , and 457 cm^{-1} and at 1070 , 807 , and 455 cm^{-1} for $y=0.36$ and 0.42 , respectively. The shift of the peaks to lower wave numbers with increasing y has been observed before and is due to the increasing replacement of O by the less electronegative Si in $\text{Si}-\text{O}_n\text{Si}_{1-n}$ ($4 \geq n \geq 0$) tetrahedral units.¹³ With increasing T , the peaks shift to larger wave numbers due to the precipitation of the excess Si and the

formation of a stoichiometric SiO_2 phase in both materials. In particular, the peak corresponding to the Si–O–Si stretching mode is seen to reach the same peak position of 1094 cm^{-1} in both samples, indicative of a similar $\alpha\text{-SiO}_2$ matrix being formed in both for sufficiently high annealing temperature.

As for the hydrogen, no peaks due to OH or H_2O groups were detected, which means that bonded H incorporates mainly as Si–H bonds. The peak corresponding to the Si–H bending mode at about 882 cm^{-1} is observed for the as-grown materials [see Figs. 4(a) and 4(b)], which is considerably reduced after annealing at 900 and 1100°C due to the outdiffusion of excess H. A closer analysis of these spectra, however, reveals traces of the Si–H bending and stretching modes, which are absent for samples annealed in pure Ar. A detailed analysis of these traces and experiments to determine the H concentration in the annealed samples will be presented elsewhere.¹⁴

IV. DISCUSSION

Both XRD and FTIR results show the formation of an $\alpha\text{-SiO}_2$ phase for annealing in Ar or ($\text{Ar}+5\% \text{H}_2$) at 900 – 1100°C . From the XRD measurements, crystalline Si-ncls are seen to form and subsequently grow in the same temperature range. The PL from corresponding samples depends on y and on the annealing gas. The XRD data allow us to establish that the Si-ncl size increases with increasing T and y , but that it remains unchanged when Ar is replaced by ($\text{Ar}+5\% \text{H}_2$) in otherwise identical annealing treatments.

The redshift of the PL mean wavelength and the concomitant reduction of the PL intensity with increasing y for both Ar and ($\text{Ar}+5\% \text{H}_2$) annealed samples are indications that the QC effect determines to some extent the characteristics of the observed luminescence. From the Si (111) peak in the XRD scans for samples annealed at 1100°C for 3 h in either Ar or ($\text{Ar}+5\% \text{H}_2$), we estimate an upper limit for the Si-ncl mean size of about 2 nm for $y=0.36$ and a mean size of 4.5 nm for $y=0.42$ (see Table I). According to tight-binding (TB) calculations,¹⁵ such a change in size should produce a redshift of the emission wavelength by 269 nm in the QC model. This is significantly larger than the experimentally observed redshifts of 58 and ~ 133 nm for Ar and ($\text{Ar}+5\% \text{H}_2$) annealed samples, respectively. A similar conclusion is deduced from the redshift of the mean PL wavelength

TABLE I. Mean size of Si-ncls obtained from XRD measurements in $\text{Si}_y\text{O}_{1-y}:\text{H}$ films with $y=0.36$ and 0.42 and annealed at 1100°C for 3 h and the corresponding observed mean PL wavelengths for samples annealed in Ar and ($\text{Ar}+5\% \text{H}_2$) atmospheres. The numbers in the column named “Theory (TB)” represent the expected emission wavelengths corresponding to the calculated Si-ncl band gaps from Ref. 15.

y in $\text{Si}_y\text{O}_{1-y}$	Mean size (nm)	Peak position (nm)		
		Theor. (TB)	Ar atmosphere	($\text{Ar}+5\% \text{H}_2$) atmosphere
0.36	<2	<626	783	807
0.42	4.5	895	841	~ 940
	Difference	>269	58	~ 133

(not shown) that accompanies the increase of the Si-ncl mean size with temperature. We thus conclude that, in addition to QC, other mechanisms must be in operation that tend to pin the PL wavelength.

A possible effect would involve recombination through disorder-induced states, most likely at the Si-ncl/SiO₂ interface region. The strong increase of the PL intensity when Ar is replaced by (Ar+5% H₂) in the annealing indicates that defects play a significant role. Possible candidates are Si dbs, which are known to be efficient luminescence quenchers at Si/SiO₂ interfaces and favorable sites for H₂ dissociation.^{16,17} While dbs can clearly explain the intensity changes, their connection with the PL mean wavelength redshift induced by the (Ar+5% H₂) treatment is less obvious. It has been suggested in the past that large Si-ncls could have a larger probability of being deactivated by a db than the smaller ones.¹⁰ Hence, H passivation would preferentially passivate the larger Si-ncls, thus producing the redshift of the PL. If this were the only effect here, the PL mean wavelength in unhydrogenated samples should tend to be blueshifted with respect to the expected theoretical values, and the sample with larger y (i.e., larger Si-ncl mean size) should show a larger discrepancy with respect to theory. Although the PL wavelength for the $y=0.42$ unhydrogenated film is indeed slightly blueshifted with respect to the expected value, it can be seen in Table I that this is far from being the case for $y=0.36$, which shows an even larger discrepancy from the expected emission wavelength, in contrast to the above.

Therefore, a more general explanation for the results presented here would need to take into consideration the participation in the luminescence of trapped excitons at defect complexes in the SiO₂/Si-ncl interface regions, such as the Si=O double bond.¹⁸ States due to this bond are known to pin the emission energy as the Si-ncls become smaller, in consistency with our results, which show a larger pinning effect for the film with smaller y . The additional redshift that occurs when the samples are hydrogenated in (Ar+5% H₂), in turn, can be understood as preferential passivation by H of dbs in disordered Si-ncls, where radiative transitions proceed between antibonding and bonding states due to distorted Si-Si bonds.¹⁹ Transitions between such states are expected to contribute photons that are redshifted with respect to transitions in less disordered Si-ncls.²⁰

V. CONCLUSIONS

The conclusions of the present article may be drawn as follows.

- (1) Annealing of Si_yO_{1-y}:H ($y=0.36$ and 0.42) samples in (Ar+5% H₂) at $T=900-1100$ °C leads to the formation of Si-ncls embedded in an α -SiO₂ matrix. PL bands in the visible develop which are attributed to light emission from Si-ncls.
- (2) The mean PL wavelength and intensity qualitatively follow the trends expected from the QC effect. However, the mean PL wavelength changes with y and T are smaller than predicted. This discrepancy is tentatively explained by the participation in the luminescence process of excitons trapped at defect complexes.
- (3) The treatment of the samples in (Ar+5% H₂) leads to a strong increase of the PL and a skew of the PL bands to the red as compared to annealing in pure Ar. The effects are explained by the selective passivation by H of db defects near disordered Si-ncls where radiative recombination proceeds between disorder-induced states.
- (4) Annealing in (Ar+5% H₂) of as-grown Si_yO_{1-y} samples and of Si_yO_{1-y} samples previously annealed in Ar leads to qualitatively similar results, illustrating the passivating role of H. The two-step treatment [Ar, 1100 °C, 3 h followed by (Ar+5% H₂), 1000 °C, 2 h] yields a slightly more efficient passivation than any single annealing step in (Ar+5% H₂).

ACKNOWLEDGMENTS

The authors gratefully acknowledge Professor William Lennard for help with Rutherford backscattering measurements and J. Garrett for assistance with the annealing furnace. This work has been funded by the Ontario Research and Development Challenge Fund (ORDCF) under the Ontario Photonics Consortium (OPC) and by Ontario Centres of Excellence (OCE) Inc.

- ¹F. Iacona, G. Franzo, and C. Spinella, *J. Appl. Phys.* **87**, 1295 (2000).
- ²T. Roschuk, J. Wojcik, E. A. Irving, M. Flynn, and P. Mascher, *Proc. SPIE* **5577**, 450 (2004).
- ³D. Comedi, O. H. Y. Zalloum, E. A. Irving, J. Wojcik, T. Roschuk, M. J. Flynn, and P. Mascher, *J. Appl. Phys.* **99**, 023518 (2006).
- ⁴F. Iacona, C. Bongiorno, C. Spinella, S. Boninelli, and F. Priolo, *J. Appl. Phys.* **95**, 3723 (2004).
- ⁵*Silicon Photonics*, edited by L. Pavesi and D. J. Lockwood (Springer, Berlin, 2004).
- ⁶A. Puzder, A. J. Williamson, J. C. Grossman, and G. Galli, *Phys. Rev. Lett.* **88**, 097401 (2002).
- ⁷C. Ternon, C. Dufour, F. Gourbilleau, and R. Rizk, *Eur. Phys. J. B* **41**, 325 (2004).
- ⁸N. Daldosso *et al.*, *Phys. Rev. B* **68**, 095327 (2003).
- ⁹M. Lannoo, C. Delerue, and G. Allan, *J. Lumin.* **70**, 170 (1996).
- ¹⁰S. Cheylan and R. G. Elliman, *Appl. Phys. Lett.* **78**, 1912 (2001).
- ¹¹M. Boudreau, M. Boumerzoug, P. Mascher, and P. E. Jessop, *Appl. Phys. Lett.* **63**, 3014 (1993).
- ¹²J. I. Langford and A. J. C. Wilson, *J. Appl. Crystallogr.* **11**, 102 (1978).
- ¹³A. Sasella *et al.*, *J. Vac. Sci. Technol. A* **15**, 378 (1997).
- ¹⁴D. Comedi, O. H. Y. Zalloum, J. Wojcik, and P. Mascher, *IEEE J. Sel. Top. Quantum Electron.* (submitted).
- ¹⁵M. P. Persson and H. Q. Xu, *Phys. Scr., T* **101**, 147 (2002).
- ¹⁶A. R. Wilkinson and R. G. Elliman, *Phys. Rev. B* **68**, 155302 (2003).
- ¹⁷K. L. Brower and S. M. Myers, *Appl. Phys. Lett.* **57**, 162 (1990).
- ¹⁸M. V. Wolkin, J. Jorne, P. M. Fauchet, G. Allan, and C. Delerue, *Phys. Rev. Lett.* **82**, 197 (1999).
- ¹⁹D. Comedi, O. H. Y. Zalloum, and P. Mascher, *Appl. Phys. Lett.* **87**, 213110 (2005).
- ²⁰L. Liu, C. S. Jayanthi, and S. Y. Wu, *J. Appl. Phys.* **90**, 4143 (2001).